

Supporting information

The pH and Concentration Dependent Interfacial Interaction and Heteroaggregation between Nanoparticulate Zero-valent Iron and Clay Mineral Particles

Yanlong Wang[†], Kun Yang^{†,‡}, Benny Chefetz[§], Baoshan Xing[¶], Daohui Lin^{*,†,‡}

[†]Department of Environmental Science, Zhejiang University, Hangzhou 310058, China;

[‡]Zhejiang Provincial Key Laboratory of Organic Pollution Process and Control, Zhejiang University, Hangzhou 310058, China

[§]Faculty of Agriculture, Food and Environment, The Hebrew University of Jerusalem, Rehovot 76100, Israel

[¶]Stockbridge School of Agriculture, University of Massachusetts, Amherst, MA, 01003, USA

*Corresponding author: Tel.: +86 571 88982582; fax: +86 571 88982590.

E-mail address: lindaohui@zju.edu.cn (D. Lin).

Number of pages: 18

Number of figures: 17

Number of tables: 1

Section S1: Additional Details on Methods

1.1 Determination of Homoaggregation Kinetics.

Homoaggregation kinetics of CMPs were quantified by attachment efficiencies (α), which was defined as the initial aggregation rate constant normalized by the aggregation rate constant measured under diffusion-limited (fast) conditions. This value was calculated from the initial aggregation rates as follows:¹

$$\alpha = \frac{\frac{1}{N_0} \left(\frac{dD_h(t)}{d_t} \right)}{\frac{1}{(N_0)_{fast}} \left(\frac{dD_h(t)}{d_t} \right)_{t \rightarrow 0, fast}}$$

where α is the attachment efficiency, N_0 is the initial particle concentration, D_h is the hydrodynamic diameter of nanoparticles, and t is the time of aggregation. The linear regression of initial homoaggregation rate was performed over a time period in that $D_{h,t}$ reached 1.3 times or 2.0 times of the initial hydrodynamic diameter ($D_{h,0}$) of CMPs. When the homoaggregation rate was very slow, such as $D_{h,t}$ failed to reach 1.3 $D_{h,0}$, then the linear regression would be achieved over a time of 10 minutes. The CCCs is the ionic strength at which α reaches a constant value of unity.

Section S2: Additional Figures

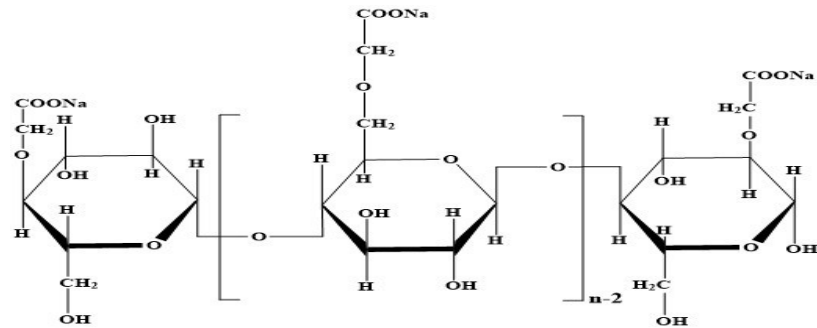


Fig. S1. Molecular structural formula of carboxymethyl cellulose.

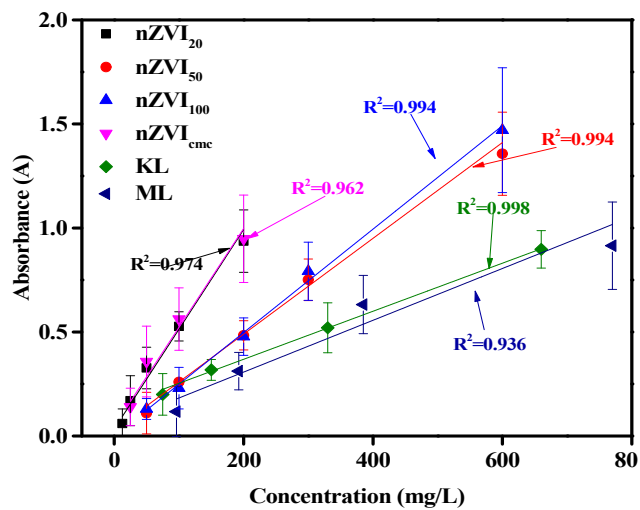


Fig. S2. The calibration curves between the absorbance at 660 nm and the concentrations of CMPs and nZVIs.

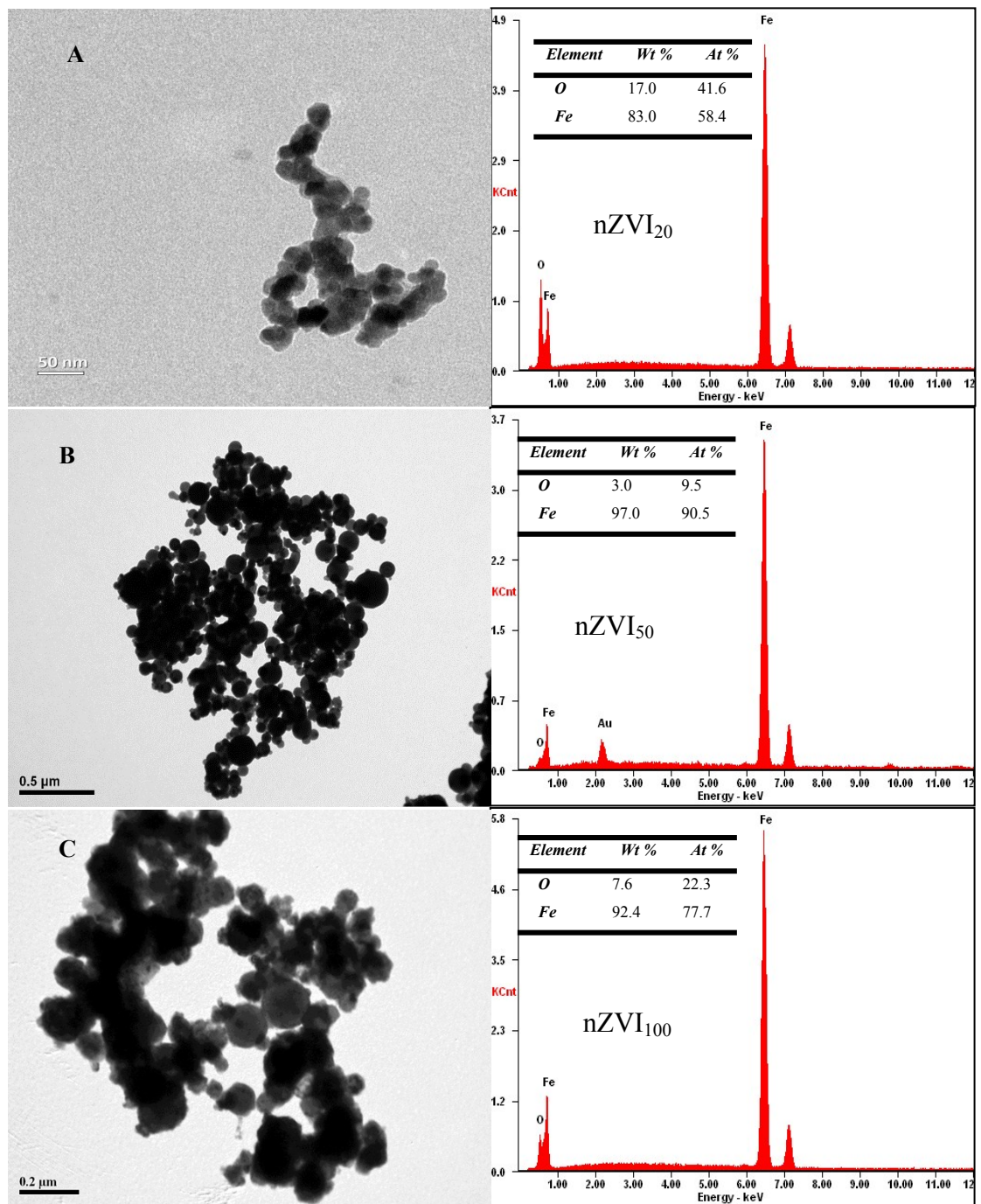


Fig. S3. TEM images (left) and EDS analyses (right) of (A) nZVI₂₀, (B) nZVI₅₀, and (C) nZVI₁₀₀; the element contents are shown in the inserts. The data were adapted from our previous paper².

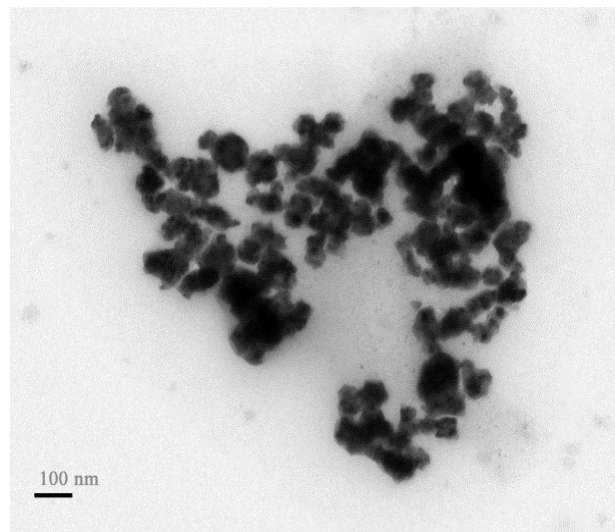


Fig. S4 TEM image of nZVI_{cmc}.

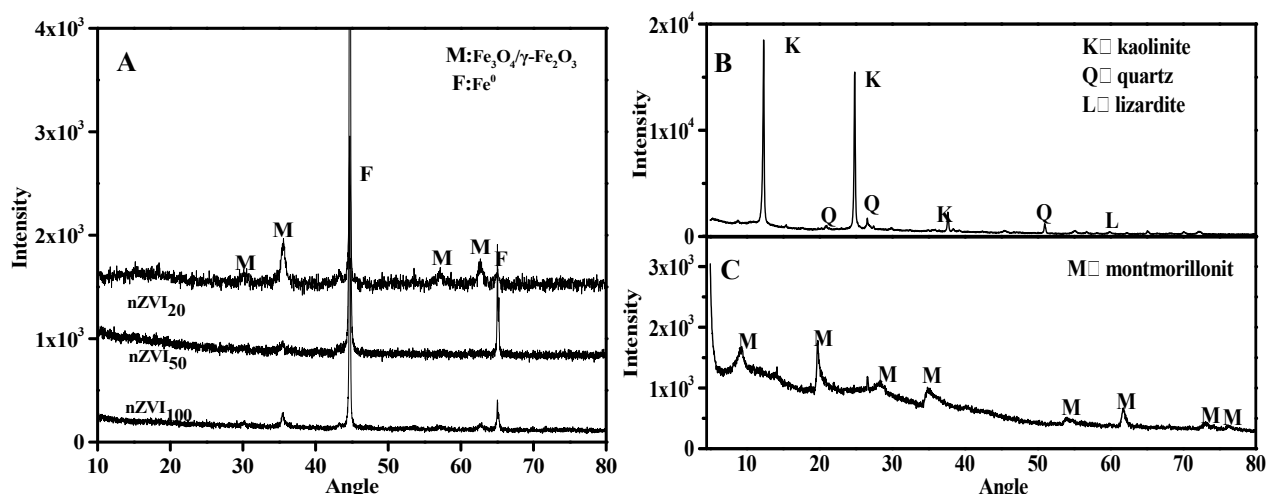


Fig. S5 The X-ray diffraction patterns of (A) nZVIs, (B) kaolinite, and (C) montmorillonite.

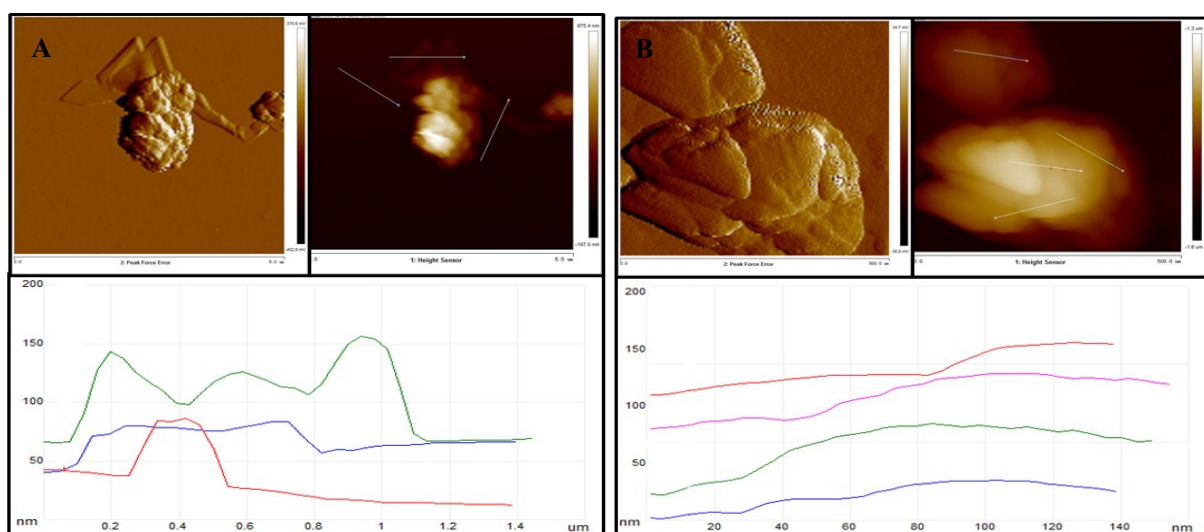


Fig. S6 AFM images (up) and height analysis (bottom) of kaolinite (A) and montmorillonite (B) particles.

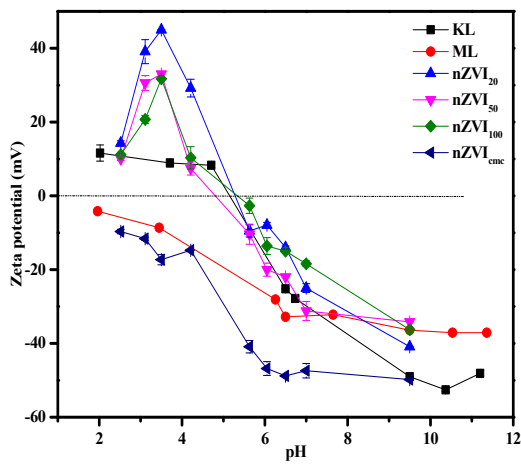


Fig. S7 ζ -potentials of nZVIs and CMPs as a function of pH with 10 mM NaCl. ML and KL represent montmorillonite and kaolinite, respectively.

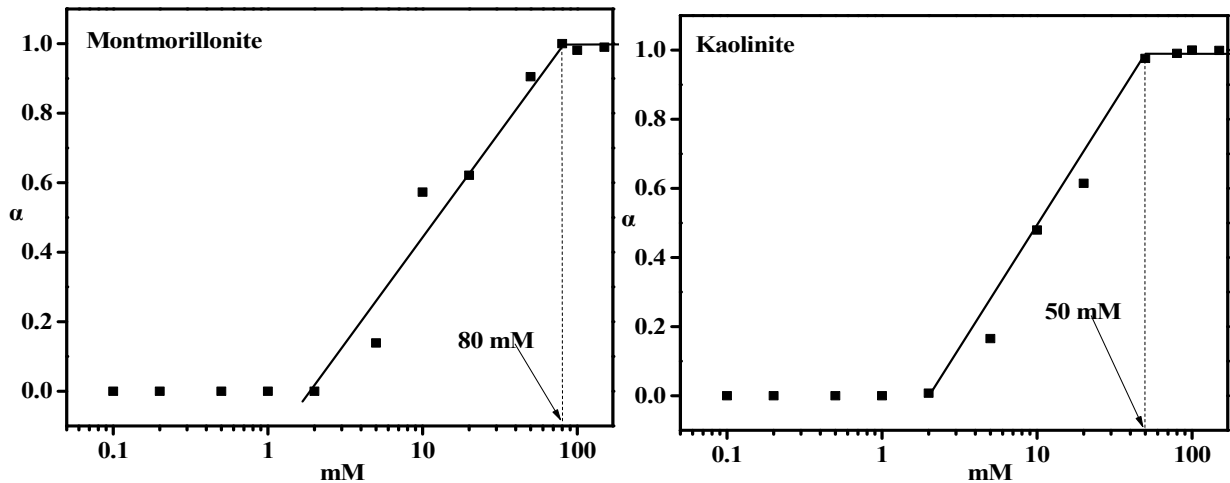


Fig. S8 Attachment efficiencies (α) of montmorillonite and kaolinite as a function of NaCl concentration at pH 6.5.

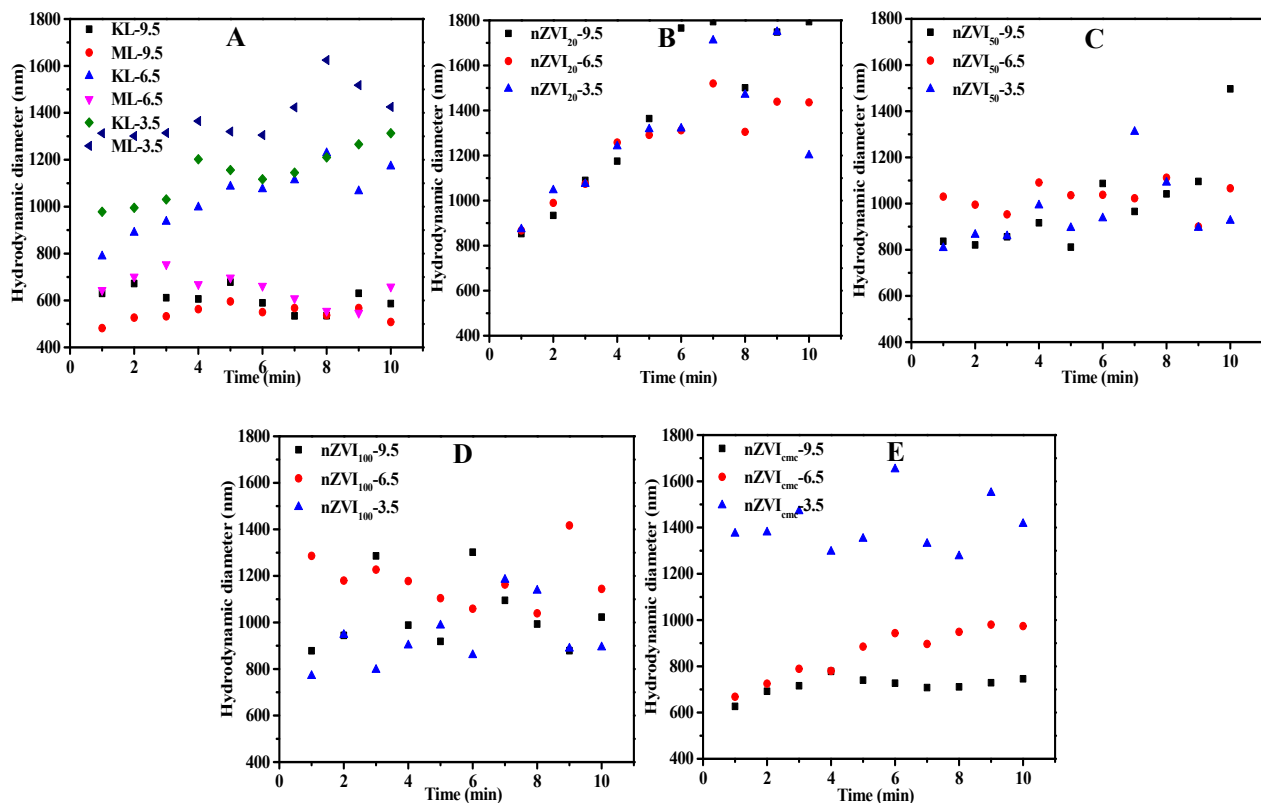


Fig. S9 Time-dependent variations in hydrodynamic diameters of nZVIs or CMPs at pH=3.5, 6.5, or 9.5 and 10 mM NaCl.

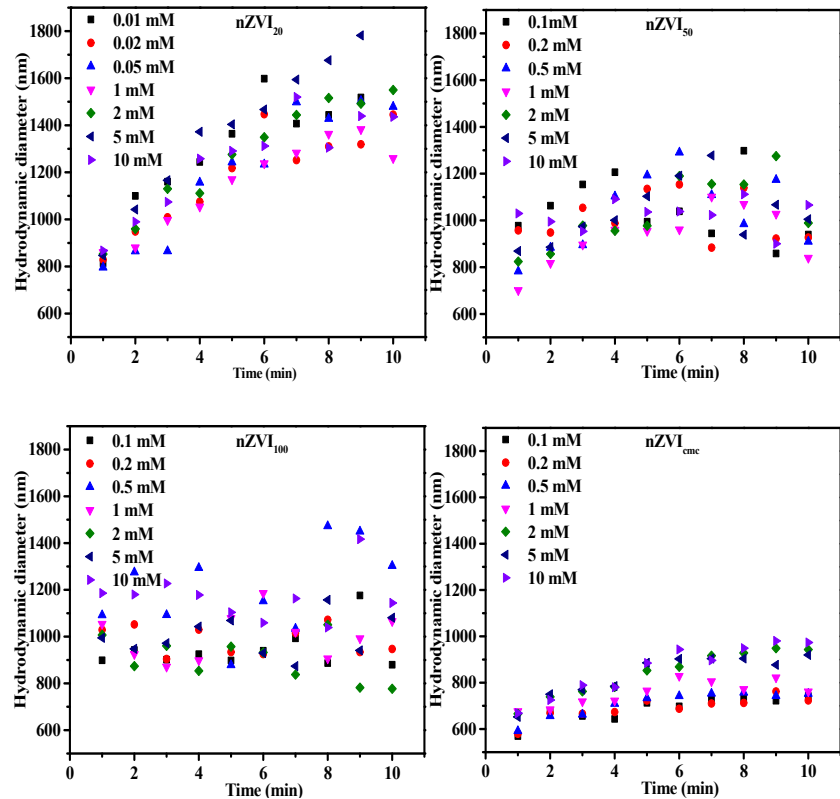


Fig. S10 Time-dependent variations in hydrodynamic diameters of nZVIs at pH 6.5 with different NaCl concentrations.

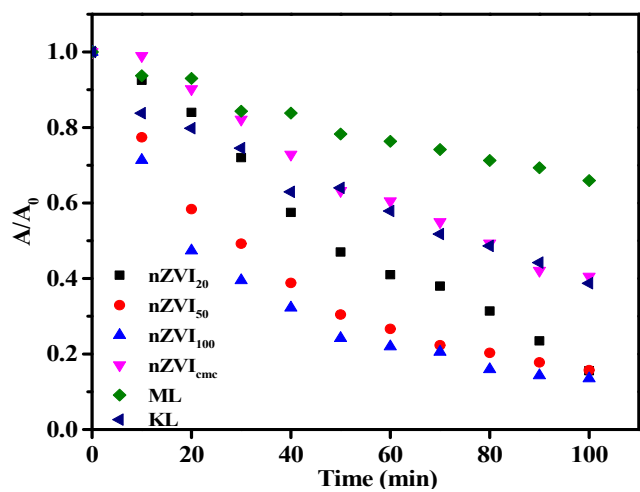


Fig. S11 Settling curves of nZVIs and CMPs at pH 6.5 and 10 mM NaCl.

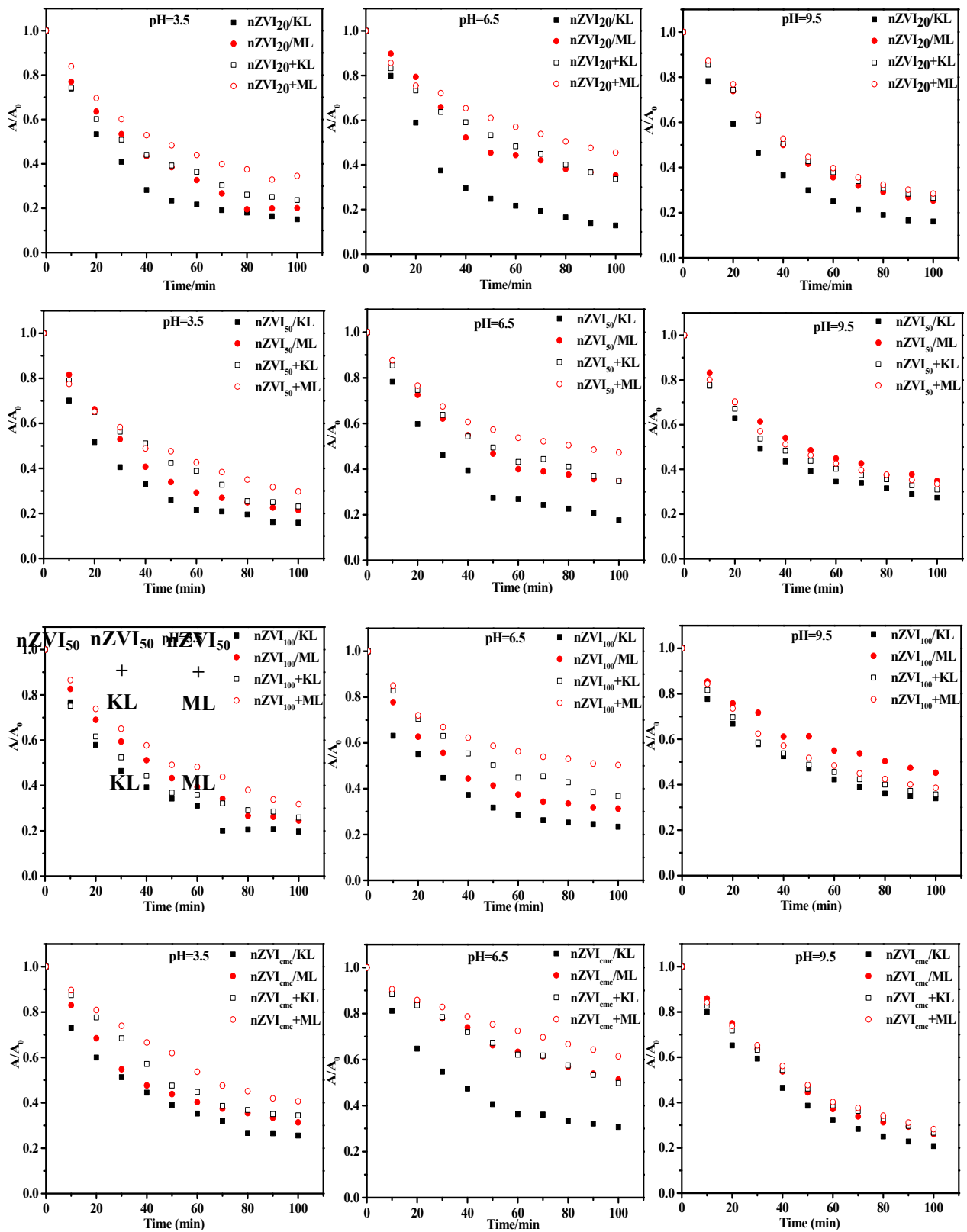


Fig. S12 (A) Additive- (nZVIs+CMPS) and co-settling (nZVIs/CMPS) curves of CMPS with nZVIs at pH=3.5, 6.5, or 9.5 and 10 mM NaCl

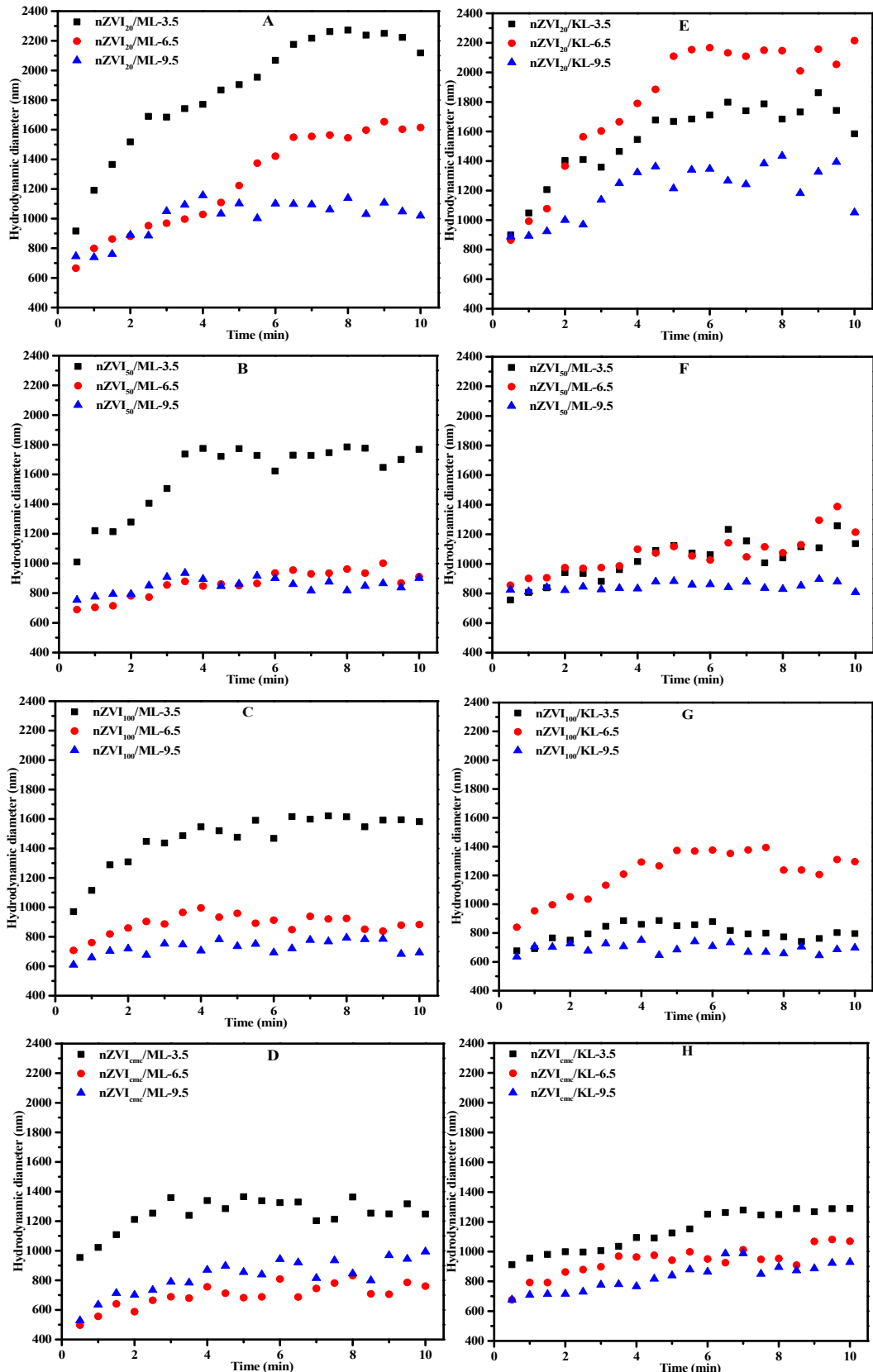


Fig. S13 Time-dependent variations of hydrodynamic diameters of nZVIs and CMPs mixtures at pH=3.5, 6.5, and 9.5 with 10 mM NaCl.

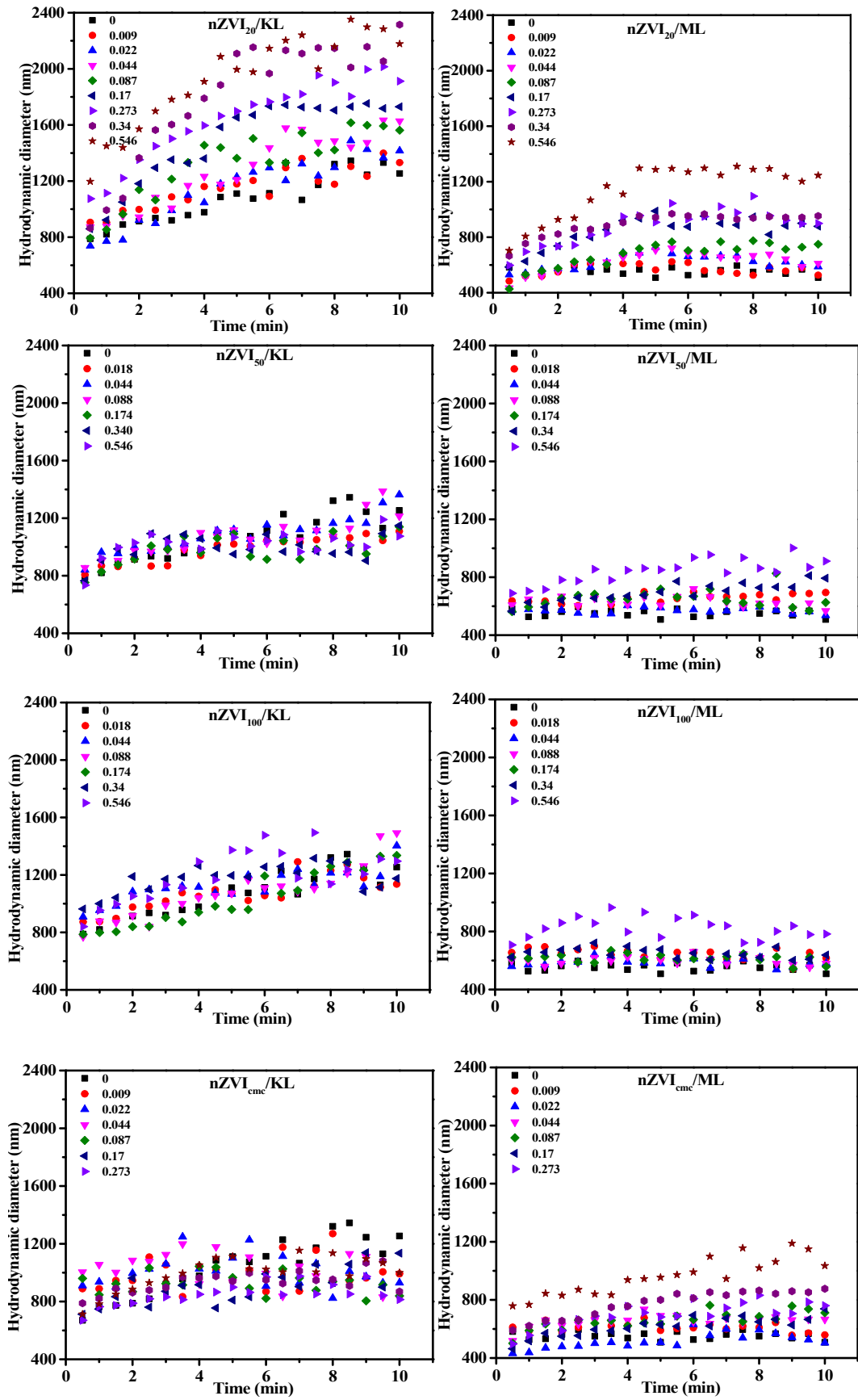
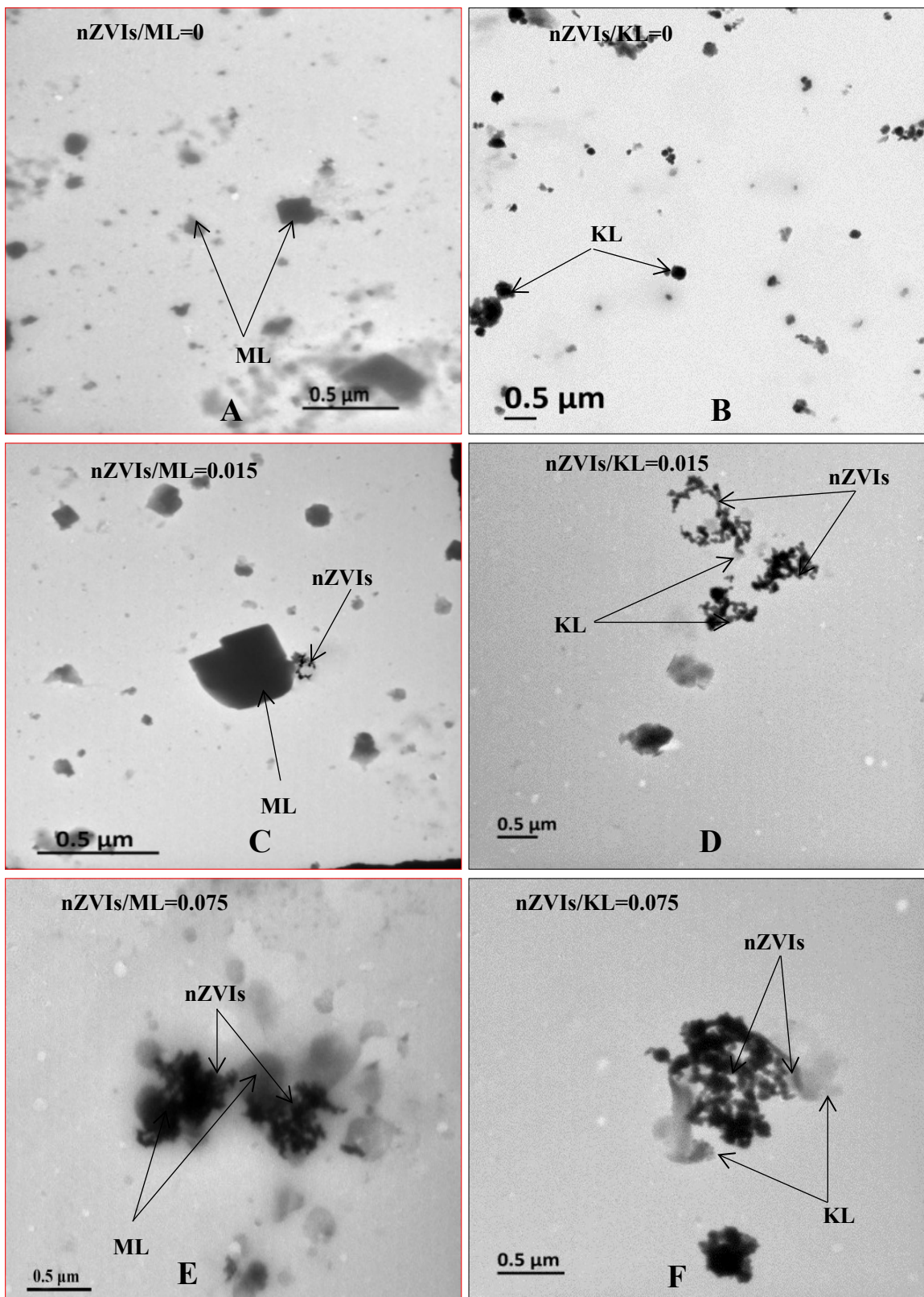
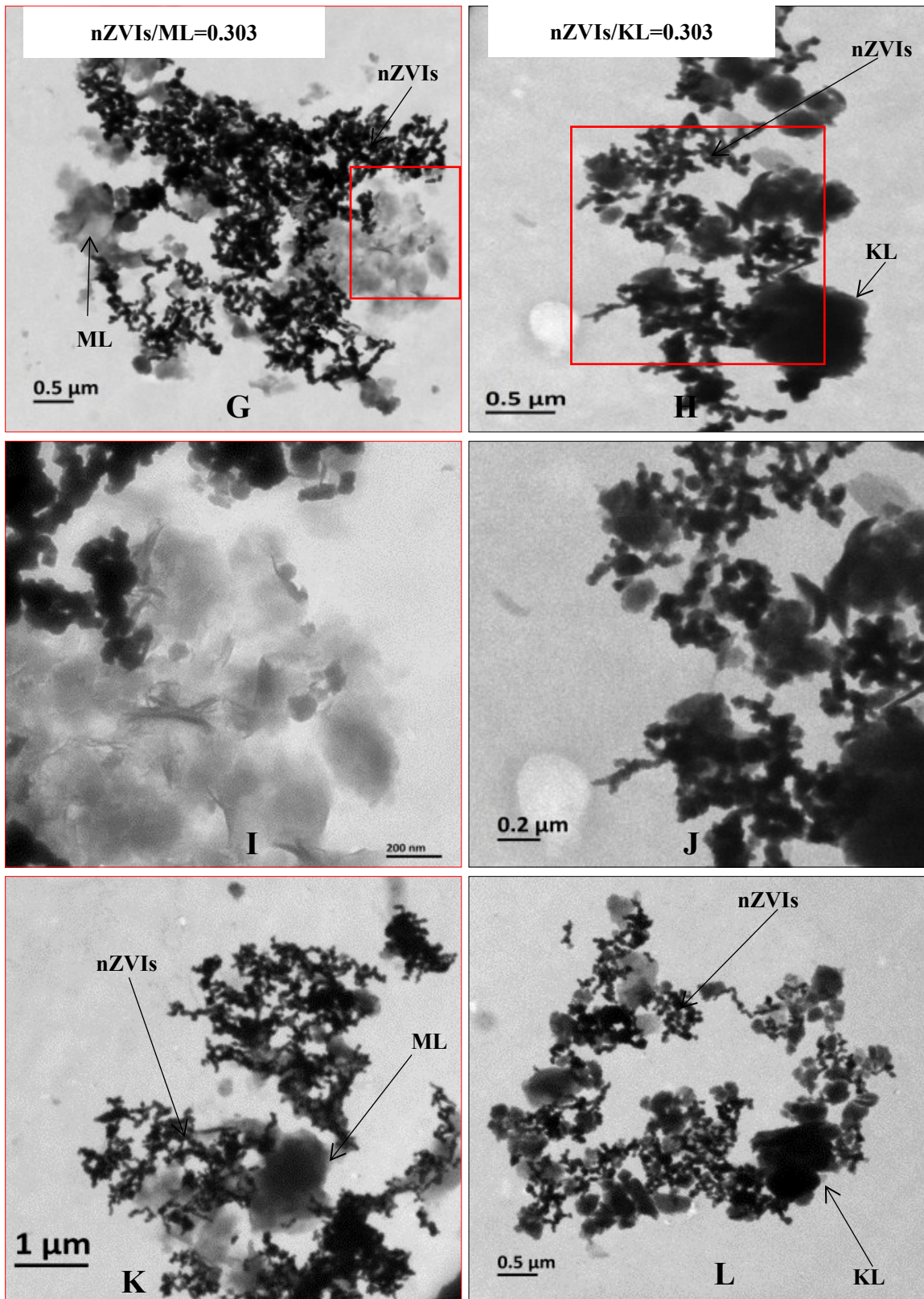


Fig. S14 Time-dependent variations in hydrodynamic diameters of nZVIs and CMPs mixtures with different mass ratios at the pH 6.5 and 10 mM NaCl.





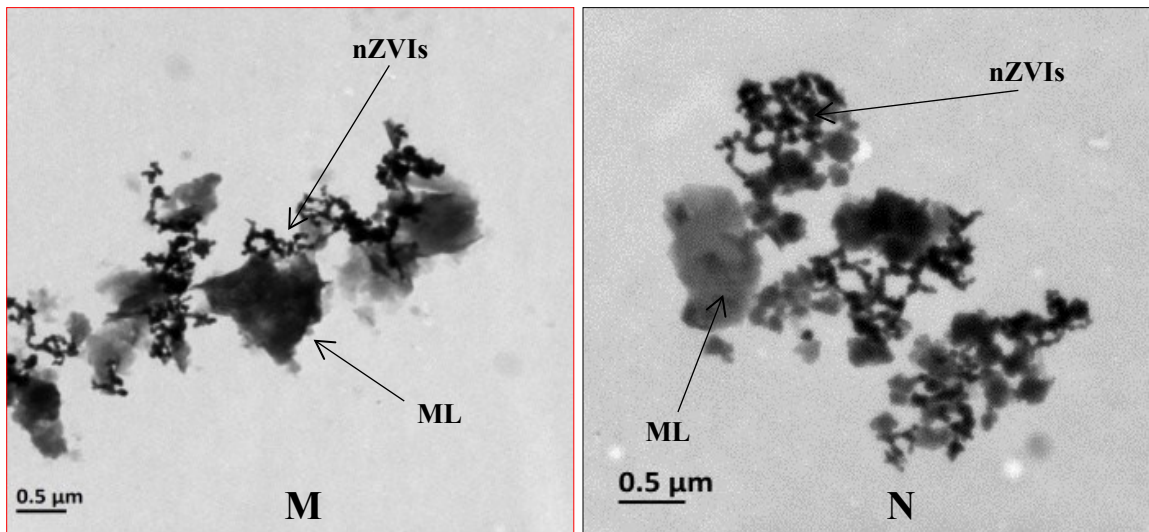


Fig. S15 Typical TEM images of heteroaggregates between nZVI₂₀ and CMPs at 10 mM NaCl:

A, C, E, and G for different mass ratios of nZVI₂₀/ML at pH 6.5; **B, D, F, and H** for different mass ratios of nZVI₂₀/KL at pH 6.5; **K and L** for 0.303 mass ratio of nZVI₂₀/ML and nZVI₂₀/KL at pH 3.5, respectively; **M** and **N** for 0.303 mass ratio of nZVI₂₀/ML and nZVI₂₀/KL at pH 9.5, respectively; **I** and **J** are enlarged images from the rectangle areas in panels **G** and **H**, respectively.

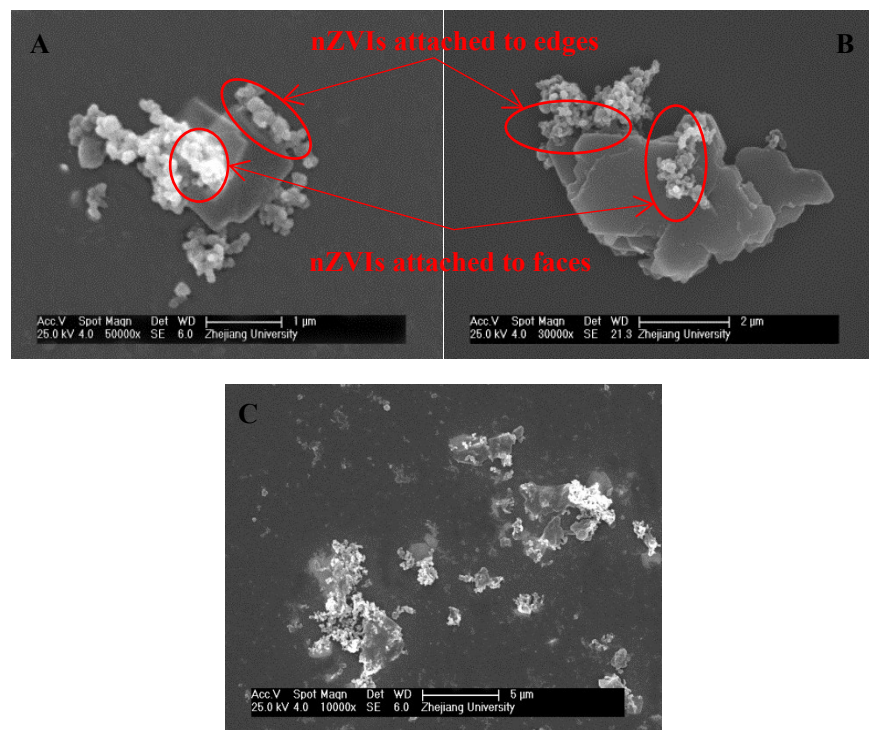


Fig. S16 SEM images of heteroaggregates of nZVI₂₀ with montmorillonite (A and C) or kaolinite (B) at pH 6.5 and 10 mM NaCl.

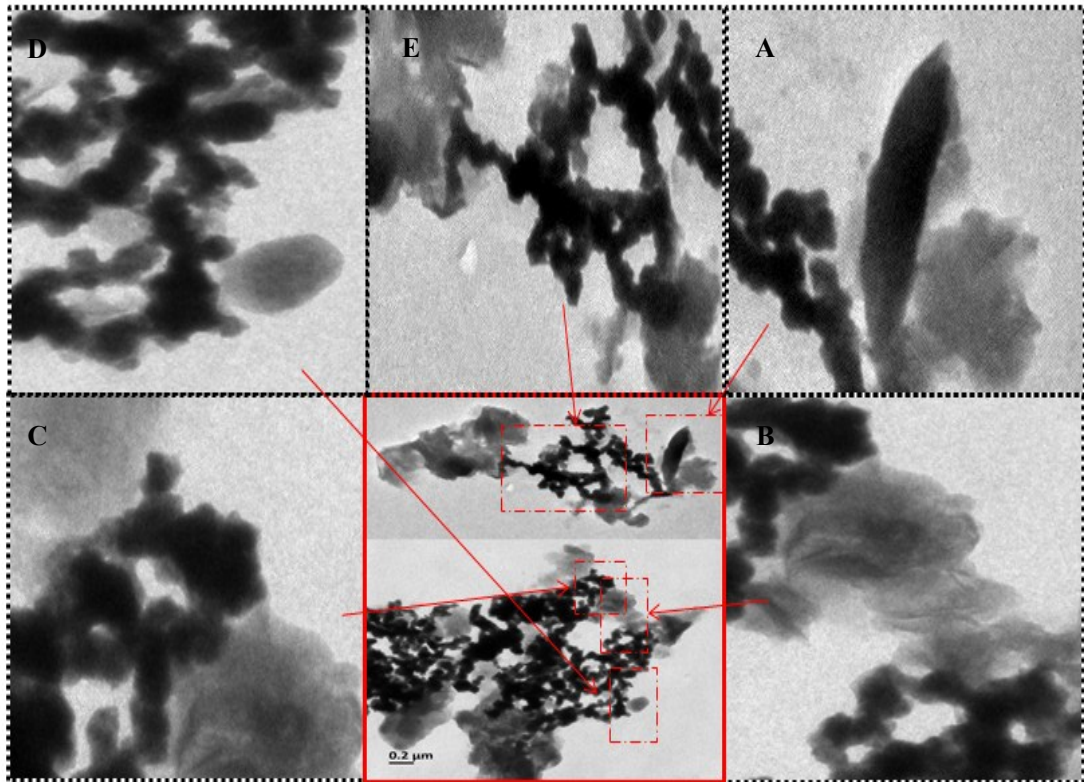


Fig. S17 TEM images of heteroaggregates in different modes. **A:** nZVI_s-CMP_s, **B:** nZVI_s-
CMP_s-nZVI_s, **C:** CMP_s-nZVI_s-CMP_s, **D:** nZVI_s-(nZVI_s/CMP_s)-nZVI_s, and **E:** CMP_s-
(nZVI_s/CMP_s/nZVI_s)-CMP_s.

Section S3: Additional Tables

Table S1 The fitted parameters of settling curves of nZVIs and CMPs.

	pH=3.5				pH=6.5				pH=9.5						
	OD ₁	SD	R ₀	R ²	ΔOD ₁	OD ₁	SD	R ₀	R ²	ΔOD ₁	OD ₁	SD	R ₀	R ²	ΔOD ₁
nZVI _{cmc} +KL	0.729	0.04	0.020	0.992	0.080	0.661	0.059	0.013	0.993	0.064	0.847	0.021	0.012	0.998	0.020
nZVI _{cmc} /KL	0.809	0.021	0.034	0.994		0.724	0.01	0.034	0.999		0.867	0.024	0.023	0.996	
nZVI _{cmc} +ML	0.718	0.054	0.013	0.996	0.128	0.505	0.048	0.012	0.993	0.150	0.852	0.025	0.011	0.998	0.022
nZVI _{cmc} /ML	0.846	0.014	0.032	0.997		0.654	0.048	0.013	0.995		0.874	0.032	0.011	0.996	
nZVI ₂₀ +KL	0.760	0.023	0.032	0.993	0.116	0.732	0.026	0.020	0.996	0.195	0.856	0.024	0.022	0.997	0.037
nZVI ₂₀ /KL	0.876	0.015	0.040	0.997		0.927	0.031	0.036	0.991		0.893	0.007	0.031	0.999	
nZVI ₂₀ +ML	0.712	0.013	0.025	0.998	0.162	0.593	0.025	0.021	0.994	0.173	0.858	0.033	0.021	0.995	0.027
nZVI ₂₀ /ML	0.874	0.026	0.027	0.995		0.766	0.044	0.024	0.983		0.885	0.033	0.022	0.995	
nZVI ₅₀ +KL	0.736	0.033	0.025	0.993	0.107	0.712	0.021	0.025	0.995	0.143	0.712	0.013	0.027	0.996	0.029
nZVI ₅₀ /KL	0.843	0.011	0.041	0.998		0.855	0.02	0.034	0.996		0.741	0.011	0.028	0.997	
nZVI ₅₀ +ML	0.699	0.026	0.029	0.991	0.162	0.564	0.009	0.026	0.998	0.179	0.693	0.012	0.026	0.997	-0.005
nZVI ₅₀ /ML	0.861	0.02	0.030	0.997		0.743	0.023	0.029	0.994		0.688	0.01	0.027	0.998	
nZVI ₁₀₀ +KL	0.840	0.014	0.027	0.998	0.023	0.652	0.015	0.028	0.996	0.082	0.668	0.011	0.022	0.997	0.008
nZVI ₁₀₀ /KL	0.863	0.024	0.044	0.994		0.734	0.03	0.046	0.987		0.676	0.016	0.023	0.996	
nZVI ₁₀₀ +ML	0.740	0.028	0.035	0.996	0.052	0.499	0.01	0.036	0.997	0.206	0.662	0.008	0.022	0.998	-0.073
nZVI ₁₀₀ /ML	0.792	0.021	0.037	0.997		0.705	0.011	0.037	0.998		0.589	0.025	0.020	0.992	

“/” and “+” indicates co-settling and additive-settling, respectively; ML and KL represent montmorillonite and kaolinite, respectively; SD is the standard deviation of OD₁.

References

- (1) Smith, B.; Wepasnick, K.; Schrote, K. E.; Bertele, A. R.; Ball, W. P.; O'Melia, C.; Fairbrother, D. H. Colloidal properties of aqueous suspensions of acid-treated, multi-walled carbon nanotubes. *Environ. Sci. Technol.* **2009**, *43*, (3), 819-825.
- (2) Lei, C.; Zhang, L.; Yang, K.; Zhu, L.; Lin, D. Toxicity of iron-based nanoparticles to green algae: Effects of particle size, crystal phase, oxidation state and environmental aging. *Environ. Pollut.* **2016**, *218*, 505-512.